AIAA SciTech Forum
6-10 January 2025, Orlando, FL
AIAA SCITECH 2025 Forum

10.2514/6.2025-1029

Dual-layer Capacitive Sensor for Enhanced Pressure Detection

Rishikesh Srinivasaraghavan Govindarajan[1], Forrest Dohner[3], Daewon Kim[4], Jenny Vu[5] and Foram Madiyar[6]
Embry-Riddle Aeronautical University, Daytona Beach, FL, 32114, USA

Mackenzie Tobin[2]
Virginia Commonwealth University, Richmond, VA, 23284, USA

In the realm of aerospace advancements, reliable flexible pressure sensors are indispensable for in-situ monitoring of crucial parameters such as pressure to enhance safety and efficiency. This paper presents the development of a novel piezoelectric MEMS-based pressure sensor tailored for static and dynamic applications. Featuring a dual-layer configuration, the sensor capitalizes on the synergistic advantages of soft and stretchable Polydimethylsiloxane (PDMS) layer patterned with intricate microstructures and a Polyvinylidene Fluoride (PVDF) dielectric second layer, thereby enhancing durability and sensitivity. The microstructures induce capacitance changes in response to the pressure variations, while the PVDF layer amplifies the sensor's responsiveness to minute pressure fluctuations. Fabricated using PVDF, PDMS, silver electrode (Ag), and Polyethylene terephthalate (PET) film, the sensor demonstrates flexibility, stretchable properties, and robust encapsulation. Advanced fabrication techniques are employed, including 3D printing for creating precise molds with micropatterns, electrospinning for producing PVDF layer, and spin coating for uniform layer deposition. Comprehensive static testing under various pressure conditions underscores the sensor's sensitivity, rapid response, and resilience in harsh aerospace environments. These findings highlight the efficacy of the dual-layer concept in advancing pressure measurement technologies, thereby contributing to performance optimization and structural integrity in aerospace systems.

I. Nomenclature

PVDF	=	Polyvinylidene fluoride
PET	=	Polyethylene terephthalate
PAA	=	Polyacrylic Acid
LCD	=	Liquid Crystal Display
IPA	=	Isopropyl Alcohol

II. Introduction

The demand for highly sensitive and reliable pressure sensor is increasing across various fields, including aerospace, automotive, wearable electronics, and industrial applications [1-3]. In the aerospace field, precise pressure

[1] Research Assistant Professor, Department of Aerospace Engineering.
[2] B.Sc student, Department of Biomedical Engineering.
[3] B.Sc student, Department of Aerospace Engineering.
[4] Professor, Department of Aerospace Engineering, AIAA senior member.
[5] Assistant Professor, Department of Physical Science.
[6] Assistant Professor, Department of Physical Science.

measurement is crucial for ensuring optimal performance, safety and monitoring the structures' health, given the varying pressure and loads experienced during flights. Various methods for sensor fabrication exist, categorized into resistive, piezoelectric, and capacitive principles [4-7]. While traditional pressure sensors offer functionality, they often suffer from limitations in sensitivity and power consumption, undermining their effectiveness in demanding environments.

Capacitive sensors, particularly those utilizing smart materials, operate on the principle of capacitance change proportional to the variation in electrode distance. They offer structural simplicity, low power consumption, rapid response times, and high reliability, making them ideal for converting external stimuli into measurable capacitance signals. Conventional flexible capacitive pressure sensors typically consist of an elastic dielectric layer sandwiched between flexible electrodes. Upon pressure application, the distance between the electrodes changes, thus affecting the capacitance value [8]. Manufacturing a three-dimensional (3D) structure on the dielectric layer is presently the preferred method for enhancing the compressibility and sensitivity of the pressure sensors [9]. 3D structures such as micro-pyramids or cylindrical patterns have been shown to improve the contact surface area and sensor sensitivity [10]. However, most studies have utilized single-sided structures, which are associated with limitations such as restricted compressibility, low durability, and increased viscoelastic behavior [11, 12].

This paper explores a dual-layer dielectric structure, as shown in Fig 1, combining electrospun polyvinylidene fluoride (PVDF) fibers with a soft, stretchable silicone-based polymer material micropillar array for capacitive pressure sensor. PVDF, recognized for its excellent dielectric properties, possesses a high molecular weight that facilitates the production of durable fibers, while its viscoelastic characteristics enable the formation of uniform fibers, making it an ideal material for flexible sensors [13]. Silicone based Sylgard 184, a soft and stretchable commercial polymer, enhances the mechanical flexibility and durability of the sensor. The combination of these dielectric materials improves the sensor performance, while simplifying the process compared to conventional methods. This dual-layer enables the sensor to achieve enhanced sensitivity and robust performance under varying pressure conditions. This sensor design offers significant improvements over traditional single-layer capacitive sensors and is promising for a wide range of applications, from aerospace to wearable electronics.

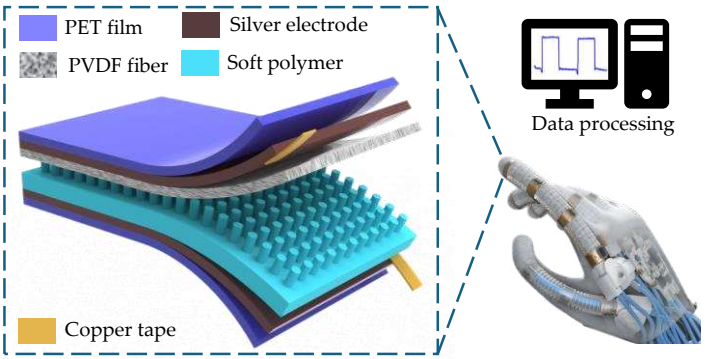

Fig. 1 Schematic representation of the dual-layer sensor construction for tactile sensing.

III. Methodology

This section outlines the fabrication methodologies for a dual-layer capacitance based pressure sensor, detailing the micropillar mold fabrication and electrospinning parameters, as shown in Fig 2.

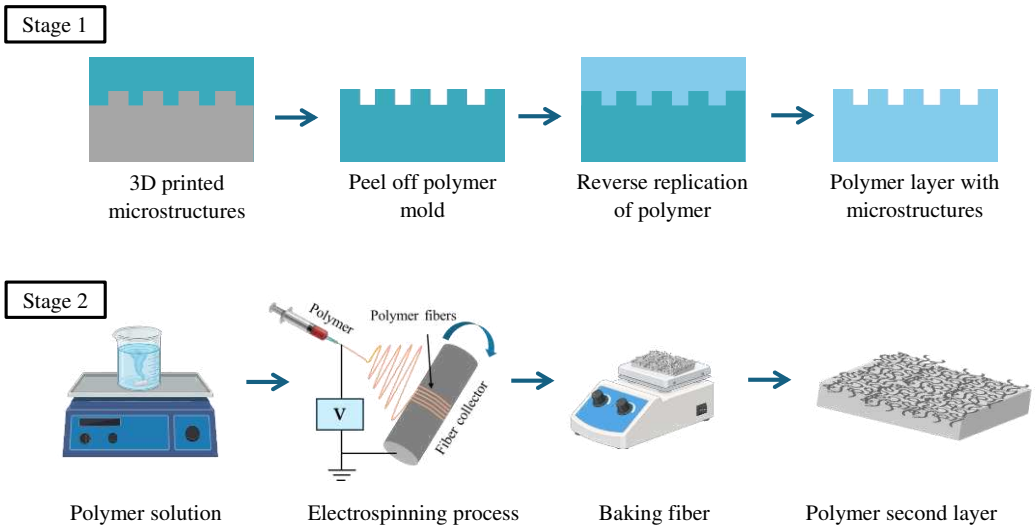

Fig. 2 Preparation process of dual-layer sensor: development stages.

A. Soft polymer synthesis

Bis (3-aminopropyl) terminated poly (dimethylsiloxane), H2N-PDMS-NH2, Mn = ~2,500, Triethylamine, ≥99.5%, anhydrous Chloroform, Methylenebis (phenyl isocyanate), Isophorone diisocyanate, and Methanol were purchased from Sigma Aldrich and used without modification. In a flame-dried round-bottom flask, 15.0 g (Mn ~2500 g/mol, 1 equivalent) of bis(3-aminopropyl)-terminated poly(dimethyl siloxane) was added to 60 mL of anhydrous Chloroform or THF at 0 °C. Then, 1.5 mL (1.8 equivalents) of Triethylamine was slowly added. Separately, a solution of 4,4'-methylenebis(phenyl isocyanate) (0.6 g, 0.4 equivalents) and isophorone diisocyanate (0.8 g, 0.6 equivalents) in 30 mL of anhydrous Chloroform or THF was prepared and added dropwise over 15 minutes to the reaction mixture, maintaining the temperature at 0 °C. The mixture was then allowed to warm gradually to room temperature and stirred overnight. The reaction was quenched with an excess of MeOH (2.3 mL) and concentrated by rotary evaporation to achieve a 20% w/w polymer solution in Choroform or THF. To reach the desired viscosity for electrospinning, an additional 9 mL of MeOH was added, and the solution was stirred for several minutes to ensure homogeneity. The soft PDMS and Sylgard 184 was characterized using Agilent Cary 630 Fourier-transform infrared (FTIR) spectroscopy with attenuated total reflectance (ATR) [14]. Spectra were averaged over 128 scans at a resolution of 4.0 cm^{-1}.

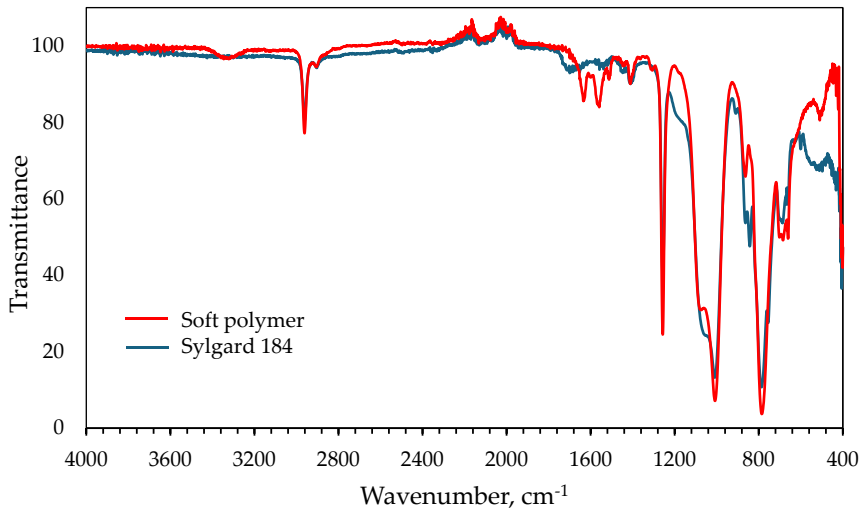

Fig. 3 FTIR spectra of the developed soft polymer compared to Sylgard 184.

As shown in Fig 3, IR spectroscopy confirmed the absence of the stretching vibration νNCO of free isocyanate groups, which typically appear around 2265 cm^{-1}. The successful synthesis of PDMS-based poly(urea)s was validated by the presence of characteristic urea peaks: 3250–3400 cm^{-1} for antisymmetric and symmetric νN-H stretching vibrations, and 1500–1700 cm^{-1} for the urea amide I and amide II regions. The amide I band (1630–1640 cm^{-1}) primarily arises from νC=O coupled with νC-N stretching and δC-C-N deformation vibrations, attributed to bidentate hydrogen-bonded urea. The amide II region (1565–1570 cm^{-1}), resulting from δN-H bending and νC-N stretching vibrations [15].

B. Fabrication of first dielectric layer with integrated microstructures

The first stage involved the fabrication of a mold with microstructures using a combination of 3D printing and reverse replication process, as illustrated schematically in Fig 2 (stage 1). A 2 cm × 2 cm resin mold with micropillars (300 µm diameter and 400 µm height) was printed using a Phrozen Sonic Mini8K Liquid Crystal Display (LCD) printer. The dimensions selected considering manufacturability, provide a suitable aspect ratio for bending under pressure, influenced by material properties, while ensuring sufficient contact area. The molds with intricate structures were rinsed thoroughly with deionized (DI) water to remove any impurities/ partially cured resin and air dried for 5 minutes. Finally, the samples were treated with UV lamp for 120 seconds. Each mold (3D printed and silicon molds) was spin-coated three times with a 15 wt% polyacrylic acid (PAA) solution in isopropanol (IPA) to create a hydrophobic coating that reduces the adhesion between the molds. For each coating, 0.6 mL of solution was applied, resulting in a total of 1.8 mL per mold. The molds were allowed to rest for 30 seconds between coatings to ensure the even distribution of the solution, followed by baking at 70 °C for 10 minutes to ensure the solution was fully dried/ cured onto the molds after each coating cycle. After the final coating, the 3D printed mold was inserted into the silicon mold and polymer candidates (Sylgard 184 (10:1) and synthesized soft polymer) were poured into the mold assembly. The setup was degassed at room temperature for 15 minutes to remove potential air bubbles, and the polymer were cured overnight at room temperature. Upon demolding, the polymer structure with uniform distributed holes was obtained. This polymer mold was further spin-coated with PAA and baked under identical parameters. Additional polymer material was poured on top of the mold, degassed and cured overnight. This resulted in a polymer mold integrated with well-defined micropillars. In terms of mechanical properties, which play a role in pressure sensing, the Sylagard 184 (10:1) exhibits a tensile strength of 5.5 MPa and an elongation of 200 % [16]. The synthesized soft polymer was characterized, showing a modulus of 0.45 MPa and an elongation of more than 475 %, indicating that it is notably softer compared to Sylgard 184.

On the other hand, PET film was submerged into isopropanol for 30 seconds and is rinsed with DI water and blow-dried to ensure the complete removal of surface contaminants. The silver paint with an acrylic binder was blade cast to the PET film, and before solidification of the polymer layer, the PET with conductive silver layer was pressed and let cure until the polymer layer was fully solidified. Then, the polymer layer with microstructures was carefully peeled off, completing the first dielectric layer in the sensor development.

C. Second dielectric layer preparation and assembly procedure

The second dielectric layer was fabricated using electrospinning of PVDF solution. To prepare the solution, 1.8 g of PVDF powder was gradually added to 6 mL of dimethylformamide (DMF), and the mixture was stirred at 70 °C for 4 hours on an Incu-shaker to achieve homogeneity. After cooling to room temperature, 10 mL of acetone was added dropwise while stirring for 2 hours at 25 °C to adjust the solution's viscosity. The formation of the Taylor cone at the needle tip is crucial for controlled fiber deposition in the electrospinning process. To ensure consistent cone formation, the key parameters, including the applied voltage and flow rate were optimized. Several variations of these parameters were tested to achieve the optimal fiber formation. The prepared PVDF solution was loaded into a 10 mL syringe, connected to a 1/16" ID × 1/8" OD tubing, and mounted on a NE-4000 syringe pump, which was set to a flow rate of 1 mL/hr. An 18-gauge needle was positioned 10 cm above a rotating collection drum. The substrate for fiber collection were 2 cm × 2 cm PET films, pre-coated with ~25 µm of silver electrode. These films were taped onto aluminum foil and placed on the rotating drum.

A high voltage of ~10.02 kV was applied to the needle to initiate the electrospinning process, creating a Taylor cone, while the collector drum was set to rotate at 250 RPM. The electrospinning process lasted for 5 minutes, after which the voltage, syringe pump, and collector were turned off sequentially. The electrospun fibers were then placed on a hot plate at 60 °C for 5 minutes to facilitate the evaporation of residual DMP and acetone. This process was repeated to ensure the deposition of sufficient amount of fibers, as shown in Fig 2 (stage 2).

After stacking the dual-layer, the entire setup was encapsulated with Kapton tape to provide electrical insulation and also protects from external environment, ensuring that the conductive layers are protected from unintended short circuits or interference. Copper tape was then connected to the silver electrode, allowing for accurate capacitance

measurements. This configuration was linked to an LCR meter to record capacitance changes under various loading and unloading pressures.

IV. Results and Discussion

A. Working mechanism of dual-layer concept

In this study, the dual-layer structure combines electrospun fibers and micropillars, creating a composite dielectric layer. The electrospun fiber introduces a porous layer, while the micropillar structure adds mechanical stability. This combination enhances the sensor's ability to respond to pressure changes while ensuring the structural integrity of the sensor.

The working principle is based on the parallel plate capacitance equation, given by: $C = (\varepsilon_r.\varepsilon_0.A)/ d$, where C is the capacitance; A is the area of the electrodes; ε_r is the relative dielectric constant; ε_0 is the dielectric constant value in free space, and d is the distance between the electrodes. The dielectric constant in this case is a cumulative value, determined by the combined combinations of the electrospun PVDF fibers, polymer micropillar layers, and the air present in the gaps between the fiber layers. Capacitance values were directly measured using a high precision LCR meter, allowing for precise analysis of the sensor's performance under varying pressure conditions.

To evaluate the impact of the dual-layer structure, control samples were fabricated without microstructures, and single-layer dielectric films were produced using polymers (Sylgard 184 and soft synthesized polymer). These comparisons enabled a deeper understanding of the improvements achieved with the dual-layer design.

B. Dual-layer structural layout inspection

The structural integrity of the dual-layer capacitance pressure sensor is assessed using optical and scanning electron microscope (SEM), focusing on both the micropillar layers and electrospun fiber. Fig 4 presents the micropillar layer, fabricated using Sylgard 184 and a soft synthesized polymer, which provides mechanical support and tension for the sensor. Optical microscopy images (Fig 4) reveal a uniform pillar structure, demonstrating the successful replication of the intended pillar shape, along with flexibility and uniformity. A key challenge during the reverse replication process was ensuring that the effectiveness of the spin coated hydrophobic layer and reproducibility, which prevented the polymer from adhering well to the master mold, a critical factor for achieving the final pillar structure. Despite this, the final micropillar layer shows the expected flexibility and uniformity, ensuring the sensor's durability and reversibility under cyclic pressure.

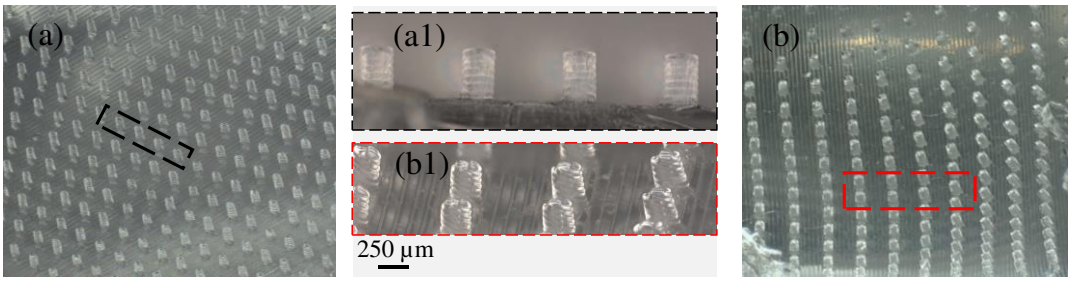

Fig. 4 Optical images of the polymer layer with micropillars (a) Sylgard 184 and (b) soft polymer.

The silver electrodes, with a measured sheet resistance of 0.017 ± 0.003 ohm/sq, ensure excellent conductivity for accurate and reliable capacitance measurements. The use of silver electrode at thin dry film thickness (~25 µm) on the PET substrate provides efficient electrical contact and minimizes signal loss, which is essential for reliable sensor performance. The silver electrode also exhibits superior environmental aging stability and scratch resistance, making it suitable for long term applications requiring durable and consistent performance. The electrospun fiber layer, shown in Fig 5, exhibits uniform fiber morphology. The fibers, ~20 µm thick with a diameter range of 0.8-1.5 µm are critical for forming micro gaps that enhance the sensor's sensitivity to small pressure variations. Challenges like fiber agglomeration were observed during the electrospinning process, requiring careful parameter optimization (e.g., applied voltage and flow rate). The final fiber configuration successfully meets design expectations, ensuring that the capacitance response is primarily influenced by dielectric changes caused by pressure-induced deformation.

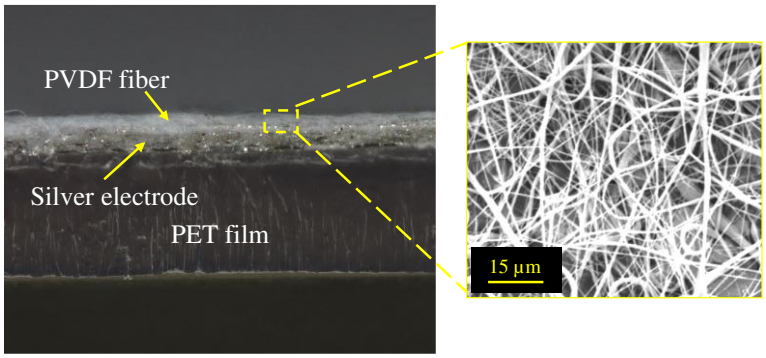

Fig. 5 Cross-sectional view of the second dielectric layer with magnified view of the electrospun fiber.

C. Validation of pressure sensing performance

To assess the effectiveness of the dual-layer pressure sensor, the performance was evaluated under controlled conditions using an experimental platform. The applied pressure was varied incrementally, and the corresponding capacitance changes were recorded with a high-precision LCR meter. This study specifically examined the pressure response in the range of 1-7 kPa and compared the dual-layer configuration against a single-layer counterpart to highlight the improvements in sensitivity and linearity.

The experimental results, illustrated in Fig 6, confirm a consistent and uniform increase in capacitance with applied pressure for all the combinations, particularly reflecting the excellent linearity and stability of the dual-layer configuration for both the polymers used in this study. The deformation behavior of the dual-layer sensor was analyzed in two distinct stages. During the initial stage, minimal pressure caused the PVDF electrospun fiber network to compress, expelling the trapped air and reducing the dielectric layer thickness. This reduction in the separation distance between the electrodes caused an increase in capacitance. In the subsequent stage, the micropillars deformed substantially by tilting and bending due to the selected aspect ratio, further enhancing the sensor's pressure response.

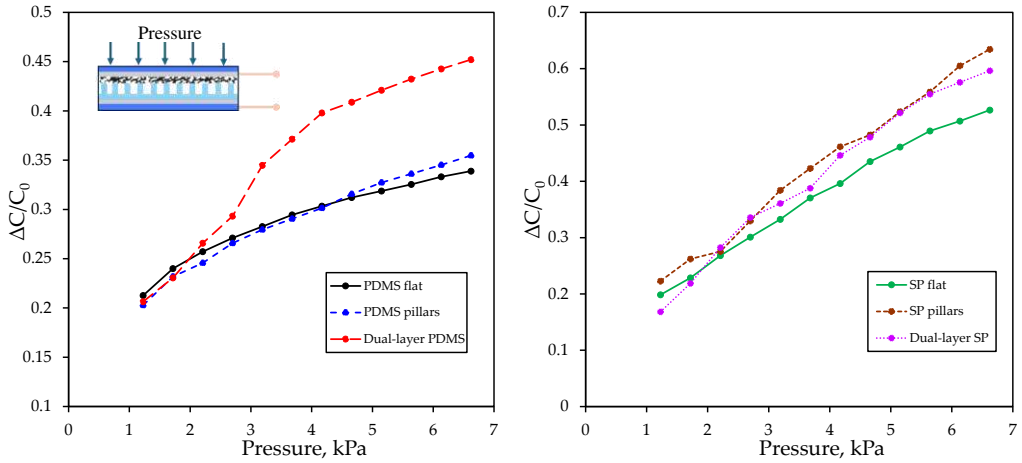

Fig. 6 Pressure detection setup with dual layer sensor mounted on a testing stage with LCR meter.

A comparative analysis revealed a notable improvement from single-layer to dual-layer configurations for both polymer materials. For Sylgard 184, the sensitivity increased from 0.0217 kPa^{-1} to 0.0473 kPa^{-1}, reflecting a substantial 118% increase. Similarly, the soft polymer demonstrated a sensitivity increase from 0.0627 kPa^{-1} to 0.0796 kPa^{-1}, corresponding to 27% increase. In the low-pressure regime, among the two polymers, the soft polymer based dual-layer sensor displayed enhanced sensitivity of 0.0796 kPa^{-1} and linearity of 0.985 due to its increased ability to adapt to subtle deformations.

Furthermore, the microstructured soft polymer pillars in the dual-layer provided an increase in the contact area between the electrodes and the dielectric, resulting in pronounced capacitance change. However, at pressures exceeding 8 kPa, the sensor response plateaued as the structural deformation approached its mechanical limit. The

synthesized soft polymer in the dual-layer system was more flexible than the Sylgard 184 material, which could be a contributing factor to the sensor's reduced ability to withstand higher pressures. While Sylgard 184 exhibited superior durability and maintained a reliable response at higher pressure ranges, the softer polymer could not maintain a similar level of resilience under these conditions. This behavior was observed both in the dual-layer and single-layer configurations, indicating that the soft polymer is optimal for sensing lower pressure ranges, where its flexibility provides significant advantages. These findings are supported by sensitivity calibration curves and summarized in a comparative Table 1 that showcases the enhanced performance of the dual-layer sensor. For high pressures, future designs could incorporate different optimal polymer molecular weights or strategies to extend the operational range. The results underline the tunability of the proposed design, making it suitable for a range of applications requiring variable pressure sensitivities. Additionally, the hybrid microstructure of the dual layer demonstrated a robust capacity to endure pressures beyond its standard operating range, offering strong protection against mechanical overload and maintaining functional integrity.

Table. 1 Sensitivity values of different pressure sensor combinations.

Sample		**Sensitivity, kPa^{-1}**	**% increase**
Sylgard 184	No microstructures	0.0217	-
	Microstructures	0.0268	23.5
	Dual-layer	0.0473	117.9
Soft polymer	No microstructures	0.0627	-
	Microstructures	0.0777	23.9
	Dual-layer	0.0796	26.9

V. Conclusion

This study demonstrates the significant enhancement in the performance of a dual-layer capacitive pressure sensor, combining electrospun PVDF fibers with a soft silicone-based polymer micropillar array. The dual layer design exhibits an improved sensitivity of 0.0796 kP^{-1} in the low-pressure regime. These results highlight the advantages of the dual-layer approach, offering a significant step forward in the development of flexible, high-performance pressure sensors. Future work will focus on validating the sensor under dynamic pressure conditions and integrating wireless data readout capabilities, further broadening its applicability in real-world scenarios. The findings suggest that this design is well-suited for applications in aerospace, healthcare, and wearable electronics, paving the way for more reliable and sensitive pressure sensing technologies.

Acknowledgments

This material is based upon work supported in part by the National Science Foundation under Grant No. 2050887 and 2347094. The opinions, findings, and conclusions, or recommendations expressed are those of the author(s) and do not necessarily reflect the views of the National Science Foundation. This project was partially supported by the National Aeronautics & Space Administration through the University of Central Florida's NASA FLORIDA SPACE GRANT. The authors would like to acknowledge Mr. Michael C. Ricciardella and Mr. Rutveek Inagawale for their assistance with a portion of the electrospinning process.

References

[1] Javed, Y., Mansoor, M., and Shah, I. A. "A review of principles of MEMS pressure sensing with its aerospace applications," *Sensor Review*, Vol. 39, No. 5, 2019, pp. 652-664. doi:https://doi.org/10.1108/SR-06-2018-0135.

[2] Kim, Y., and Oh, J. H. "Recent Progress in Pressure Sensors for Wearable Electronics: From Design to Applications," *Applied Sciences*; Vol. 10, No. 18, 2020. doi:https://doi.org/10.3390/app10186403.

[3] Seesaard, T., and Wongchoosuk, C. "Flexible and Stretchable Pressure Sensors: From Basic Principles to State-of-the-Art Applications," *Micromachines*; Vol. 14, No. 8, 2023. doi:https://doi.org/10.3390/mi14081638.

[4] Kim, T. Y., Suh, W., and Jeong, U. "Approaches to deformable physical sensors: Electronic versus iontronic," *Materials Science and Engineering: R: Reports*, Vol. 146, 2021, p. 100640.

doi:https://doi.org/10.1016/j.mser.2021.100640.
[5] Cao, C., Zhou, P., Wang, J., Liu, M., Wang, P., Qi, Y., and Zhang, T. "Ultrahigh sensitive and rapid-response self-powered flexible pressure sensor based on sandwiched piezoelectric composites," *Journal of Colloid and Interface Science*, Vol. 664, 2024, pp. 902-915.
doi:https://doi.org/10.1016/j.jcis.2024.03.099.
[6] He, J., Zhang, Y., Zhou, R., Meng, L., Chen, T., Mai, W., and Pan, C. "Recent advances of wearable and flexible piezoresistivity pressure sensor devices and its future prospects," *Journal of Materiomics*, Vol. 6, No. 1, 2020, pp. 86-101.
doi:https://doi.org/10.1016/j.jmat.2020.01.009.
[7] Srinivasaraghavan Govindarajan, R., Ren, Z., Melendez, I., Boetcher, S. K., Madiyar, F., and Kim, D. "Polymer Nanocomposite Sensors with Improved Piezoelectric Properties through Additive Manufacturing," *Sensors*, Vol. 24, No. 9, 2024, p. 2694.
doi:https://doi.org/10.3390/s24092694.
[8] Srinivasaraghavan Govindarajan, R., Ren, Z., Madiyar, F., and Kim, D. "Additive Manufacturing of Photocurable PVDF-Based Capacitive Sensor," *ASME 2023 Conference on Smart Materials, Adaptive Structures and Intelligent Systems*. Vol. ASME 2023 Conference on Smart Materials, Adaptive Structures and Intelligent Systems, Austin, Texas, USA, 11-13 September 2023.
[9] Zhao, K., Han, J., Ma, Y., Tong, Z., Suhr, J., Wang, M., Xiao, L., Jia, S., and Chen, X. "Highly Sensitive and Flexible Capacitive Pressure Sensors Based on Vertical Graphene and Micro-Pyramidal Dielectric Layer," *Nanomaterials*; Vol. 13, No. 4, 2023.
doi:https://doi.org/10.3390/nano13040701.
[10] Srinivasaraghavan Govindarajan, R., Stark, T., Madiyar, F., and Kim, D. "On the performance of PVDF based piezoelectric sensor with microstructures," *SPIE Smart Structures + Nondestructive Evaluation*. Vol. 12486, SPIE, 2023.
[11] Joo, S., Han, J. Y., Seo, S., and Kim, J.-H. "Patterning Techniques in Coplanar Micro/Nano Capacitive Sensors," *Micromachines*; Vol. 14, No. 11, 2023.
doi:https://doi.org/10.3390/mi14112034.
[12] Bijender, and Kumar, A. "Recent progress in the fabrication and applications of flexible capacitive and resistive pressure sensors," *Sensors and Actuators A: Physical*, Vol. 344, 2022, p. 113770.
doi:https://doi.org/10.1016/j.sna.2022.113770.
[13] Srinivasaraghavan Govindarajan, R., Rojas-Nastrucci, E., and Kim, D. "Surface Acoustic Wave-Based Flexible Piezocomposite Strain Sensor," *Crystals*, Vol. 11, No. 12, 2021, p. 1576.
doi:https://doi.org/10.3390/cryst11121576.
[14] Madiyar, F., Vu, J. M. B., Ricciardella, M., Dohner, F., Shivakumar, J., and Rojas, E. "Electrospinning Thin Films of Stretchable and Self-Healing PDMS," *2024 IEEE Aerospace Conference*. 2024, pp. 1-7.
[15] Kang, J., Son, D., Wang, G.-J. N., Liu, Y., Lopez, J., Kim, Y., Oh, J. Y., Katsumata, T., Mun, J., Lee, Y., Jin, L., Tok, J. B. H., and Bao, Z. "Tough and Water-Insensitive Self-Healing Elastomer for Robust Electronic Skin," *Advanced Materials*, Vol. 30, No. 13, 2018, p. 1706846.
doi:https://doi.org/10.1002/adma.201706846.
[16] Sikulskyi, S., Ren, Z., Mekonnen, D. T., Holyoak, A., Srinivasaraghavan Govindarajan, R., and Kim, D. "Additively manufactured unimorph dielectric elastomer actuators: Design, materials, and fabrication," *Frontiers in Robotics and AI*, Vol. 9, 2022.
doi:https://doi.org/10.3389/frobt.2022.1034914.